ZIBELINE INTERNATIONAL™ PUBLISHING

Water Conservation and Management (WCM)

DOI: http://doi.org/10.26480/wcm.01.2026.155.162

ISSN: 2523-5664 (Print)
ISSN: 2523-5672 (Online)
CODEN: WCMABD

RESEARCH ARTICLE

APPLICATION OF CELLULAR AUTOMATA FOR SOIL INFILTRATION ASSESSMENT IN SUPPORT OF WATER CONSERVATION: A CASE STUDY OF THE KALISARI SUB-WATERSHED

Istika Nita[a]*, Aditya Nugraha Putra[a], Priska Ayuningtyas[b], Dinna Hadi Sholikah[c], Sugeng Prijono[a]

[a]Soil Science Department, Faculty of Agriculture, Universitas Brawijaya, Malang, Indonesia
[b]Agroecotechnology Study Program, Faculty of Agriculture, Universitas Brawijaya, Malang, Indonesia
[c]Department of Agrotechnology, Faculty of Agriculture, Universitas Pembangunan Nasional Veteran Jawa Timur, Surabaya, Indonesia
Corresponding Author Email: istika.nita@ub.ac.id

Article History:

Received 27 February 2026
Revised 20 March 2026
Accepted 25 March 2026
Available online 03 April 2026

ABSTRACT

Part of the hydrological cycle, soil infiltration serves as a pivotal indicator for evaluating water availability potential within the Kalisari Sub-watershed. By employing modeling techniques to analyze its spatial distribution, this study aims to forecast the watershed's capacity to sustain agriculture by 2030. The research area spans approximately 5,000 hectares, encompassing five distinct land uses: P1 (mahogany-coffee agroforestry), P2 (pine-coffee agroforestry), P3 (shrub), P4 (dryland), and P5 (paddy fields). A comprehensive investigation, involving 43 observation points, was conducted to facilitate modeling and accuracy assessment through techniques such as Kappa Accuracy Assessment, implemented using QGIS 2.18 and ArcGIS 10.4. Precipitation data obtained from a rainfall simulator were utilized to simulate rainfall intensity and measure soil infiltration rates. Correlation-regression analyses were performed using R Studio, employing the Pearson correlation method to ascertain the relationship between soil parameters and infiltration. Projections indicate that by 2030, the soil infiltration rate within the Kalisari Sub-watershed is expected to be classified as "very fast" (>250 mm h^{-1}). Kappa accuracy modeling demonstrated an accuracy rate of approximately 82.74%, validating the reliability of the modeling approach. Furthermore, the study identified a significant interaction between land use patterns and soil properties, resulting in a dynamic decrease in infiltration rates of approximately 13.47% during 2021 to 2030 within the Kalisari Sub-watershed. However, the decrease is not significant because the lowest infiltration rate is around 328.51 cm h^{-1}, thus indicating that the hydrological capacity of the entire watershed land is likely to remain stable under the projected land use scenario and is able to support agricultural systems until 2030.

KEYWORDS

Agriculture, Cellular Automata, Rainfall Simulator, Sentinel 2a, Water Resources.

1. INTRODUCTION

Precise water management constitutes a critical measure in addressing the challenge of water scarcity while facilitating an understanding of soil's water retention capacity (Mathur and Damle, 2021). Within watershed ecosystems, soil infiltration rate stands as a key component of the hydrological cycle (Wang et al., 2015a). (Besar et al., 2013) elucidate soil infiltration as a multipart process involving water ingress into the soil, subsequent movement, and alterations in storage dynamics. Notably, organic matter input (Tamod et al., 2020) and transitions between land uses (Ren et al., 2020) emerge as influential factors affecting infiltration rates.

Changes in land use and land productivity can detrimentally affect water absorption and storage capacity in a region (Wicaksono et al., 2022). However, the introduction of organic matter into soil has been recognized to enhance soil pore space, thereby improving soil properties and consequently influencing water storage potential through the infiltration process (Machiwal et al., 2006). The movement of water within the landscape, governed by potential energy gradients, underscores the possibility of surface runoff in the absence of adequate ground cover (Wang et al., 2015b). Therefore, the application of organic matter to soil is anticipated to play a pivotal role in stabilizing soil aggregates (Thomas et al., 2020), promoting more uniform water distribution within the soil, and mitigating surface runoff.

The Kalisari Sub-watershed, characterized by its transition from dryland to agricultural use dominated by annual crops, faces challenges regarding water resource sustainability. A critical parameter for assessing water resource availability is soil infiltration capacity, which serves as an indicator of water storage potential (Morrison et al., 2020). Analyzing infiltration values enables the identification of trends, facilitating model preparation and trend analysis (Morbidelli et al., 2018).

Analyzing trends derived from model preparation results facilitates the estimation of soil infiltration. Modeling soil infiltration capability serves as an initial stride toward understanding the propensity of agricultural lands to sustain their agricultural systems by gauging water absorption

Quick Response Code	Access this article online	
	Website: www.watconman.org	**DOI:** 10.26480/wcm.01.2026.155.162

Cite The Article: Istika Nita, Aditya Nugraha Putra, Priska Ayuningtyas, Dinna Hadi Sholikah, Sugeng Prijono (2026). Application of Cellular Automata for Soil Infiltration Assessment in Support of Water Conservation: A Case Study of The Kalisari Sub-Watershed. *Water Conservation and Management*, 10(1): 155-162.

potential and its future availability (Saputra et al., 2021). Within the Kalisari sub-watershed, characterized by dryland dominance, discerning the factors influencing soil infiltration necessitates a comprehensive understanding of soil characteristics across various regions. The model's outcome manifests as a map delineating land use patterns and forecasts infiltration distribution from 2015 to 2030.

The assessment of land use change trends employs spectral transformation methodologies, leveraging Sentinel 2A imagery to analyze land cover dynamics spatially and temporally. Prior model preparations involved processing via multiple transformations including NDSI, SAVI, OSAVI, NDWI, and MSAVI. The Normalized Difference Soil Index (NDSI) scrutinizes land cover variations by incorporating seasonal land surface temperature conditions (Tariq et al., 2020). Meanwhile, the Soil Adjusted Vegetation Index (SAVI) mitigates soil brightness effects to estimate actual vegetation cover per location (Islam et al., 2021). Optimized Soil Adjusted Vegetation Index (OSAVI) demonstrates prowess in predicting land cover amidst significant soil background variability (Mao et al., 2020), while MSAVI, an evolution of SAVI, presents a simplified algorithm independent of landline principles. MSAVI's utility spans soil organic matter analysis, drought monitoring, and vegetation cover assessments, including leaf area index (LAI) estimation and pasture yield evaluations (Binte et al., 2021). NDWI maximizes water reflection utilizing green wavelengths to minimize vegetation-related interference, with positive values indicative of optimized water detection (Morsy and Mashaan, 2022). Determinant coefficients derived from transformation index formulas evaluate the relevance of these transformations, constituting the base model (Zokaib and Naser, 2012). Spectral transformations encompassing plant, soil, and water indices are poised to furnish accurate assessments of land cover conditions.

The modeling approach employs the cellular automata (CA) method, renowned for its capacity to forecast changes in land area with respect to infiltration tendencies (Indarto et al., 2020). Leveraging spatial analysis, CA facilitates the examination of prevailing land use conditions and enables the projection of future scenarios. Extant research underscores the efficacy of CA in simulating spatial and temporal variations in infiltration levels over distinct periods, predicated on rainfall influences (Ji et al., 2020). While numerous studies have scrutinized disparities in infiltration capacity across diverse land uses, comprehensive mapping of infiltration distribution and its future projections remains relatively scarce. Thus, this study endeavors to assess changes in land use infiltration rates, validate the accuracy of land use models for 2030 utilizing CA, and ascertain the Kalisari sub-watershed's agricultural support capacity based on projected infiltration distribution data for 2030.

2. Material And Methods

2.1 The Study Area

The study was conducted within the Kalisari Sub-watershed, situated in the Karangploso District of Malang Regency, on the South Slope of Mount Arjuna. The study included 43 observation points distributed across five dominant land use types: P1 (Mahogany–Coffee Agroforestry), P2 (Pine–Coffee Agroforestry), P3 (Shrub), P4 (Dryland), and P5 (Paddy Fields). The sampling points were selected using a stratified survey approach, ensuring that each major land use class within the Kalisari sub-watershed was proportionally represented. The spatial distribution of the sampling points was designed to capture variability in vegetation cover, soil conditions, and topographic characteristics, thereby improving the representativeness of infiltration measurements across the watershed. Research site selection and soil sampling sites were determined using survey methods, referencing Sentinel 2A imagery.

Soil property analysis was performed at the Laboratory of Soil Physics and Chemistry within the Department of Soil, Faculty of Agriculture, Universitas Brawijaya. The research spanned from June to October 2021, structured into four primary sub-activities: pre-survey and survey activities, observations (including land cover analysis, sampling, and soil infiltration measurements using a rainfall simulator), laboratory analyses, and map preparation to generate modeling outputs.

2.2 Infiltration model development

The development of the infiltration model in this study adopts the cellular automata method, incorporating factors influencing land use changes, such as the presence of settlements or built-up areas and accessibility via roads (Dimara et al., 2020). Utilizing Sentinel 2A imagery, an unsupervised classification approach is employed to generate maps, leveraging the spatial resolution capabilities of Sentinel-2A, deemed conducive for precise land use classification (Indarto et al., 2020). Infiltration data undergoes processing and spatialization within a geospatial information system, facilitating the correlation analysis of MSAVI, NDSI, NDWI, SAVI, and OSAVI transformation indices with the distribution of infiltration data and soil inspection outcomes within the Kalisari sub-watershed area. A schematic representation of the infiltration development model is illustrated in Figure 1.

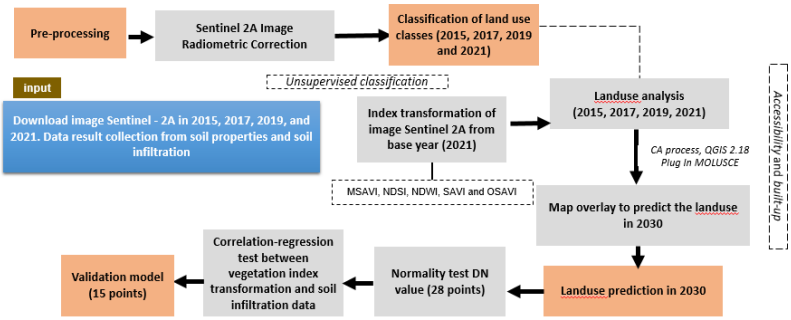

Figure 1: Scheme for modelling soil infiltration in Kalisari sub-watershed

Spatial driving factors influencing infiltration patterns include vegetation indices (MSAVI, SAVI, OSAVI), soil exposure index (NDSI), and moisture index (NDWI). The relative influence of these variables was evaluated using Pearson correlation analysis, and variables with stronger relationships with infiltration were considered more influential in the modeling framework.

2.3 Classification of Land Use and Modeling of Cellular Automata

entinel 2A imagery from 2015, 2017, 2019, and 2021 is obtained based on satellite recording timings. Following image download, geometric and radiometric adjustments are conducted to ensure accuracy. If discrepancies in research sample placement arise, geometric correction is applied. Atmospheric correction, serving as the radiometric adjustment, aims to mitigate interference from objects or clouds, such as scattered light. The Focus 2016 software is utilized for this radiometric correction procedure (Ma et al., 2021). Subsequent steps involve image cropping and band organization, with a focus on arranging band 432 (true color) within the Sentinel 2A image.

Cellular Automata (CA) modeling is employed for land use prediction in future scenarios. In natural sciences and geography, the CA approach simplifies the creation of models for intricate spatial processes. Essentially, CA operates by establishing discrete processing mechanisms, wherein each element or object, known as an automaton, undergoes transitions or movements. This mechanism exhibits adaptability in response to external inputs and a predefined set of rules. The CA model assumes that land use transitions occur based on neighborhood interactions and spatial driving factors, where the state of each cell is influenced by surrounding cells and transition probabilities derived from historical land use patterns (Munthali et al., 2020).I n this study, the CA model assumes that land use transitions occur through local neighborhood interactions, where the state of each cell is influenced by surrounding cells and by spatial driving factors. The transition rules were

derived from historical land use changes observed between 2015, 2017, 2019, and 2021, while spatial drivers including distance to roads, proximity to settlements, and environmental indices (MSAVI, NDSI, NDWI, SAVI, OSAVI) were used to influence the probability of land use transition.

2.4 Transform Map for the Water and Soil Availability Index

The index transformation procedure was subsequently conducted on the previously acquired Sentinel image through analysis using the QGIS program. Table 1 presents the spectral indices used to represent soil moisture conditions, vegetation cover, and soil exposure, which are key variables influencing infiltration processes. MSAVI, SAVI, and OSAVI were selected because these indices reduce soil background effects in areas with sparse vegetation cover, while NDWI represents surface moisture conditions and NDSI captures soil exposure characteristics that may influence infiltration variability.

Table : Formula for the Water and Soil Index (indexdatabase.de)

Indeks	Rumus / formula
NDSI	$\frac{\rho MIR - \rho NIR}{\rho MIR + \rho NIR}$
NDWI	$\frac{\rho Green - \rho NIR}{\rho Green + \rho NIR}$
SAVI	$\frac{800\ nm - 670\ nm}{800\ nm + 670\ nm + L}(1 + L)$, L= 0.5
OSAVI	$(1 + Y)\frac{800\ nm - 670\ nm}{800\ nm + 670\ nm + L}$, Y= 0.16
MSAVI	$\frac{(2NIR + 1 - \sqrt{((2NIR + 1)^2 - 8(NIR - Red))}}{2}$

In this study, the Normalized Difference Soil Index (NDSI), Normalized Difference Water Index (NDWI), Soil Adjusted Vegetation Index (SAVI), Optimized Soil-Adjusted Vegetation Index (OSAVI), and Modified Soil Adjusted Vegetation Index (MSAVI) were generated utilizing the index transformation method applied to Sentinel 2A images. The Raster Calculator tool within ArcMap via ArcToolbox is employed to process the NDSI, NDWI, SAVI, OSAVI, and MSAVI indices. Subsequently, spatial analysis tools and map algebra techniques are utilized to generate new raster data (Rahmasari and Rustanto, 2022).

2.5 Survey and soil sampling

The observation plots measured 20 × 20 m, representing the dominant land use condition at each sampling location. Within each observation plot, a 15 m^2 soil sampling sub-plot was established for infiltration testing and soil property measurements. Undisturbed soil samples, extracted from the topsoil layer, are utilized for analyzing bulk density, soil permeability, and aggregate stability. Conversely, disturbed soil samples are employed for analyzing texture, total porosity, organic matter content, and particle density. The delineation of the soil sampling area corresponds to the Sentinel 2A image.

2.6 Soil infiltration measurement

Infiltration rates were measured using a portable rainfall simulator equipped with a full-cone nozzle system. The rainfall intensity was calibrated to 70 mm h^{-1}, representing the average high-intensity rainfall events in the Karangploso region based on regional rainfall statistics. Each simulation was conducted for 30 minutes over a 0.5 m × 0.5 m plot area. The rainfall simulator frame was installed vertically above the test plot with a 1.5 m nozzle height to ensure uniform drop formation. Runoff water was collected through a bordered metal frame installed around the plot to minimize edge effects and lateral flow losses. The infiltration rate (RI) is calculated using the formula:

$$RI\,\frac{(mm)}{(hour)} = \frac{V\ (mm^3)}{L\ (mm^2).t\ (h)}$$

Where RI represents rain intensity (mm h^{-1}), V denotes the volume of runoff and sediment storage tank (mm^3), A signifies the area of the test object (mm^2), and t indicates time (h). Rainfall was applied using a portable rainfall simulator equipped with a full-cone nozzle system. The rainfall intensity was calibrated to 70 mm h^{-1}, representing high-intensity rainfall events commonly observed in the Karangploso region. Each rainfall simulation was conducted for 30 minutes over a 0.5 m × 0.5 m experimental plot. The simulator nozzle was positioned at a height of 1.5 m above the soil surface to allow uniform raindrop formation. A metal frame border was installed around the experimental plot to minimize edge effects and lateral water losses during runoff collection. Rainfall uniformity was tested prior to the experiment using the Christiansen Uniformity Coefficient (CU) to ensure spatially consistent rainfall distribution across the experimental plot. The simulated rainfall intensity was compared with regional rainfall records from the Karangploso meteorological station to ensure that the applied rainfall conditions represent local rainfall characteristics (Iserloh et al., 2013).

Soil properties analysis: Soil samples were collected from the surface to a depth of 20 cm in the form of whole and crushed soil samples for analysis of soil texture (pipette method), soil bulk density (g cm^{-3}), soil specific gravity (g cm^{-3}), soil porosity (%), aggregate stability (wet sieve method, MWD), soil permeability (cm h^{-1}) and soil organic matter (%).

Data analysis :The paired t-test was applied to evaluate temporal differences in spectral indices between observation years at the same sampling locations, allowing assessment of whether significant changes occurred between time periods, facilitated through the Genstat 10.4 application. Subsequently, the data is input into the attribute table within ArcMap for further analysis.

Accuracy test:Model outputs were validated by comparing predicted infiltration distribution with observed field measurements using the Kappa Accuracy Assessment in QGIS 2.18, employing the Kappa Accuracy Assessment test (McHugh, 2012). Subsequently, the strength of accuracy is assessed through Kappa coefficients, as outlined in Table 2.

Table 2: Kappa accuracy coefficient

K	Strength of Agreement
<0.2	Poor
0.21- 0.4	Fair
0.41 –0.6	Moderate
0.61 – 0.8	Good
0.81 – 1.00	Very good

A subset of 15 observation points (approximately 34% of the total dataset) was randomly selected as independent validation samples, while the remaining points were used for model development. The proportion of validation samples follows commonly applied spatial modeling practices, where 30–40% of the dataset is reserved for model validation to ensure an unbiased accuracy assessment. These validation points were spatially distributed across the different land use types to ensure that the Kappa accuracy assessment reflects the variability of infiltration conditions within the watershed (Verma et al. 2020).

2.7 Correlation-regression test

The collected data underwent statistical analysis employing the Pearson correlation methodwithin the R Studio software. This comprehensive analysis aimed to ascertain the influence of diverse soil parameters, such as bulk density, porosity, particle density, soil permeability, and aggregate stability, on agricultural land use and soil infiltration distribution. However, the CA model applied in this study does not explicitly incorporate external drivers such as extreme rainfall variability, land management practices, or future socio-economic changes. These factors may influence infiltration dynamics and introduce uncertainty in long-term spatial predictions.

3. Results And Discussion

3.1 Map of Land Use in the Kalisari Sub-Watershed in various index transformations

The modification of several indices, including MSAVI, NDSI, NDWI, OSAVI, and SAVI, has led to an observed increasing trend in the values of each index across the years from 2015 to 2021. The selection of spectral indices was based on their ability to represent key surface and vegetation conditions relevant to cellular automata (CA)–based landscape and environmental modeling. MSAVI, SAVI, and OSAVI were included because these soil-adjusted vegetation indices reduce the influence of soil background reflectance and provide a more stable representation of vegetation cover in areas with sparse or heterogeneous canopy conditions. NDWI was selected to capture surface moisture dynamics that influence hydrological processes and infiltration behavior, while NDSI was used to characterize soil surface conditions and potential exposure of bare soil. In

addition, soil physical parameters, bulk density, porosity, and aggregate stability, were considered because they directly control soil structure, pore connectivity, and water movement, which are critical factors influencing infiltration processes and land surface responses within CA-based environmental simulations. Prior to analysis, multicollinearity among predictor variables was evaluated using both correlation analysis and the variance inflation factor (VIF). The revised correlation matrix showed that all pairwise correlations remained below the commonly accepted threshold ($r < 0.80$), and VIF values ranged between 2.3 and 3.8, indicating the absence of problematic multicollinearity. Temporal dynamics of the indices were further examined using paired t-tests applied to the same observation points across different years, allowing the detection of statistically significant changes in vegetation and surface conditions over time while maintaining the paired structure of the dataset.

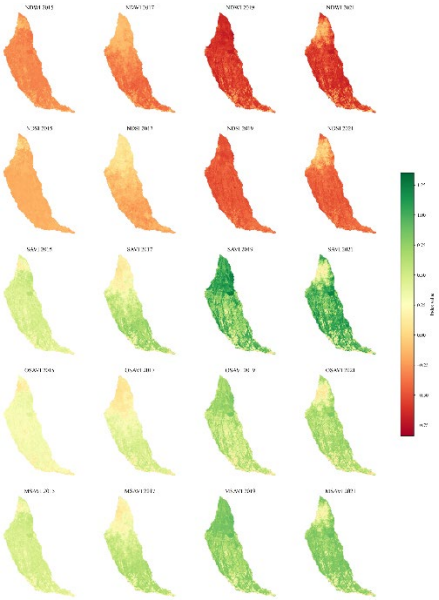

Figure 2: Vegetation Index Transformation from 2015 to 2021 (NDWI, NDSI, SAVI, OSAVI and MSAVI**)**

Based on the data analysis spanning from 2015 to 2021, it was observed that the SAVI index consistently exhibited the highest values across each year. The SAVI (Soil Adjusted Vegetation Index) algorithm was developed to mitigate the influence of soil background on canopy brightness levels, utilizing NDVI data. SAVI incorporates vegetation isoline equations derived from a first-order photon interaction model between the soil layer and canopy, alongside canopy reflectance approximation. These equations characterize vegetation under varying soil backgrounds while maintaining consistent density. The decrease in the red spectrum's contribution results in a darker soil background and a notable increase in NDSI (Normalized Difference Soil Index). This suggests that NDSI is particularly sensitive to darker soils induced by vegetation growth.

3.2 Land use changes in the Kalisari sub-watershed

Based on the land use analysis, it is evident that shrubs and dryland are the predominant land cover types within the Kalisari sub-watershed. Mahogany-coffee and pine-coffee agroforestry areas represent ecosystems characterized by minimal community intervention, rendering them favorable in ecological terms. The Kalisari Sub-watershed is geographically divided into three distinct zones: forested areas situated at elevations ranging from 1160 to 1265 meters above sea level, drylands spanning altitudes between 636 and 752 meters above sea level, and residential zones or rice fields positioned at elevations of 467 to 600 meters above sea level. The size and composition of agricultural lands significantly influence the hydrological conditions within the watershed. The sustainability of the watershed is intricately linked to the management of natural resources, particularly the biophysical conditions in the upstream regions. The land use structure comprising Natural Forest, Mahogany-Coffee Agroforestry, and Pine Coffee Agroforestry in the upstream watershed areas exhibits a well-maintained ecosystem, largely attributable to minimal community intervention in land use practices.

The land use predictions for the Kalisari watershed between 2015 and 2021 indicate that the upstream region is primarily characterized by forest land cover, encompassing both natural forest and mahogany-coffee agroforestry, while the middle segment is dominated by dryland and shrub vegetation. Conversely, the downstream area is predominantly characterized by residential land use, with limited areas allocated to paddy fields and drylands. As highlighted by (Wang et al., 2015b), the transformation of agricultural land into alternative land uses represents an inevitable and impactful change in land function.

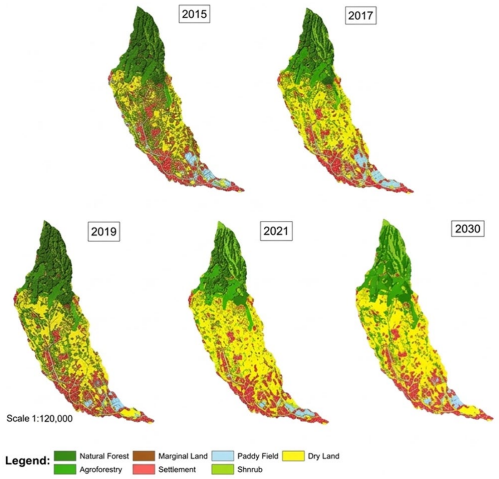

Figure 3: Landuse change in Kalisari Sub-watershed in 2015-2030

In general, the land use pattern within the Kalisari sub-watershed undergoes annual transformations, as depicted in Figure 3. Land use change refers to the transition from one land use function to another (Kusrini et al., 2016), often driven by increasing land demand from local communities. Notable changes observed over the 2015–2021 period include a decline in the utilization of paddy fields and natural forests (specifically mahogany-coffee agroforestry), juxtaposed with a consistent rise in land allocation for settlements, pine-coffee agroforestry, and scrub shrubs. Moreover, there is a discernible trend of conversion from natural forest and mahogany-coffee agroforestry to pine-coffee and shrub agroforestry during this timeframe. These shifts in land use reflect the evolving needs and priorities of the local community, underscoring the dynamic nature of land use dynamics in response to societal demands.

3.3 Cellular automata modelling

To assess the accuracy of the land use change map generated using the CA method for the year 2030, validation and accuracy tests are imperative (Fransiska and Pratomoatmojo, 2019). As elucidated by (Fardani et al., 2020), the accuracy test for the CA method serves to evaluate the error value within a model, thereby gauging its level of precision. During the attribute input stage, ArcGIS 10.4 and QGIS 2.18 are employed to compute changes in land area occurring annually. In this study, the chosen accuracy assessment method is Kappa Accuracy, facilitated by a confusion matrix, yielding results as depicted in Figure 4.

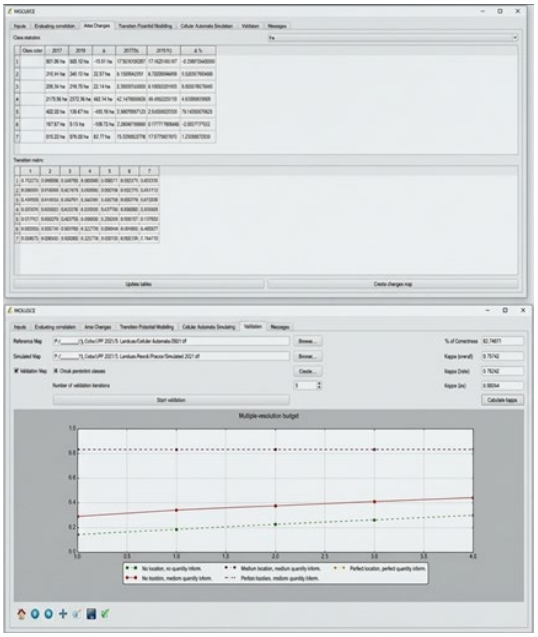

Figure 4: Automatic kappa accuracy test with MOLUSCE plugged in QGIS 2.18

A total of 15 points were selected based on the digital number value extracted from Sentinel-2A imagery. The accuracy assessment yielded a result exceeding 80%, with a correctness percentage of 82.74% (top right corner), indicating that the land use map generated using CA modeling can effectively project land use dynamics for 2030. According to (Norizah et al., 2022), CA modeling proves instrumental in making informed decisions regarding agricultural expansion, enhancing agricultural productivity, and conserving remaining forested areas over a defined timeframe. The proportion of land use exhibiting minimal changes suggests limited influence from driving factors such as accessibility and built-up land.

3.4 Prediction of land use change area in 2030

Human activities play a crucial role in driving land use transformations within the sub-watershed area, indicating a dynamic response to evolving land needs. The prediction of land use changes from 2015 to 2030 is illustrated in Fig. 5 and Table 3. This prediction method utilizes cellular automata (CA), which is a modeling approach capable of capturing the complexities of an area and forecasting land use changes based on prevailing trends (Asra et al., 2020).

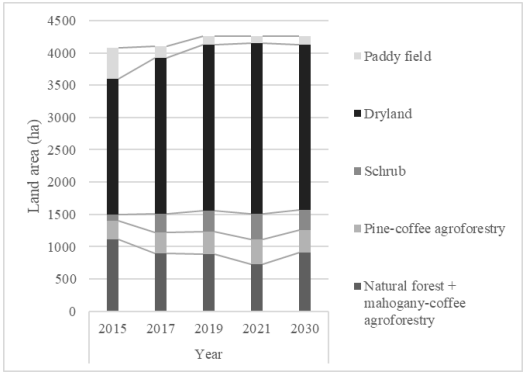

Figure 5: Diagram of predicted land area transformation over the years

Table 3 : The Kalisari Sub-watershed's landuse change from 2015 to 2030

Land use	Land area (ha)				
	2015	2017	2019	2021	2030
P1	1,118.44	901.49	885.15	722.68	904.63
P2	281.54	315.61	348.18	394.69	347.92
P3	96.09	296.56	318.7	387.76	317.33
P4	2,108.06	2,412.52	2,572.36	2,640.72	2,554.05
P5	480	179.52	136.07	107.80	136.05

**P1=Mahogany-Coffee Agroforestry, P2=Pine-Coffee Agroforestry, P3=Shrub, P4=Dryland and P5=Paddy Fields*

Dryland is projected to remain the dominant land use within the Kalisari watershed by the year 2030. Predictive modeling indicates a notable acceleration in land use changes compared to the base year of 2015. In 2030, relative to 2015, the area allocated to pine-coffee agroforestry is expected to increase to 347.92 hectares, while land dedicated to mahogany-coffee agroforestry will diminish to 904.63 hectares, with rice fields experiencing a reduction to just 136.05 hectares. The conversion of paddy fields to dry fields aims to meet the community's growing demand for vegetables, given their higher market value and easier maintenance compared to lowland rice cultivation (Machiwal et al., 2006). Additionally, the conversion of some vacant land into new residential areas reflects the expanding agricultural activities driven by community needs (Pérez-Girón et al., 2022). This shift signifies a decline in forested land area, characterized by the conversion to other land uses such as production forest or plantations. However, the area allocated to mahogany-coffee agroforestry is anticipated to exhibit a gradual increase from 2021 to 2030, suggesting efforts toward sustainable land management during this period. This phenomenon has significant implications for human activities, particularly in terms of land conversion and the establishment of settlements (Anderson et al., 2020).

The dynamics of land use change, as modeled by the CA method, are influenced by various driving factors, including socioeconomics, demographics, politics, and spatial planning. While this study primarily focuses on agricultural land, it is acknowledged that the broader context involves a multitude of complex factors that shape land using dynamics.

3.5 Prediction of soil infiltration trend

Various land uses within the Kalisari sub-watershed have exhibited dynamic changes from 2015 to 2030, as depicted in Figure 3. Notably, pine-coffee agroforestry emerged as the predominant land use with the highest infiltration capacity, except in 2015. Shrublands consistently demonstrated the highest infiltration rates, while Mahogany–Coffee Agroforestry exhibited relatively higher infiltration rates in 2017 compared with other land uses. Paddy fields and drylands, subject to intensive land management practices, may experience compaction over time. Dryland exhibited slightly lower infiltration rates (389.60 mm h^{-1}) compared to paddy fields (394.84 mm h^{-1}), while shrublands showed comparable values (392.12 mm h^{-1}). Mahogany-Coffee Agroforestry (396.23 mm h^{-1}) and pine-coffee agroforestry (397.27 mm h^{-1}) showcased relatively similar infiltration capacities. The distribution of soil infiltration across various land uses is outlined in Table 4.

Prediction models suggest an increase in infiltration rates by 2021 followed by a decline by 2030, aligning with anticipated land changes in the Kalisari Sub-watershed. The decrease in infiltration rate occurred in all land uses and was highest in shrub land use at 20.09%. This trend correlates with the observed rise in dryland (±2.7%), shrub (±21.7%), and agroforestry land (±11.8%) from the preceding year (2017). Changes in land use significantly impact soil qualities, particularly physical characteristics, consequently influencing soil infiltration dynamics (Sun et al., 2018). However, the Kalisari Sub-watershed presents distinct observations, with minimal large-scale changes in land use translating to limited variations in soil physical attributes. According to (Nita et al., 2024), soil texture and organic matter are primary determinants contributing to the classification of soil infiltration rates as very fast across the diverse land uses within the Kalisari sub-watershed.

Table 4: The Kalisari sub-watershed's rate of soil infiltration from 2015 to 2030

Land use	Infiltration rate (mm h^{-1})					% Change (2015-2030)
	2015	2017	2019	2021	2030	
P1	403.33	403.44	356.97	396.23	349.35	-13.38%
P2	402.80	400.02	357.17	397.27	353.64	-12.20%
P3	411.10	396.60	353.51	392.12	328.51	-20.09%
P4	396.81	396.88	348.26	389.60	340.73	-14.13%
P5	390.78	390.88	346.11	394.84	361.20	-7.57%

**P1=Mahogany-Coffee Agroforestry, P2=Pine-Coffee Agroforestry, P3=Shrub, P4=Dryland and P5=Paddy Fields, (-) = Percentage decrease in infiltration rate*

Soil management practices and land use activities exert a significant influence on infiltration rates by dictating the degree of disturbance experienced by the soil (Anderson et al., 2020). Across the study area, the observed infiltration rates ranged from 379.34 to 397.27 mm h^{-1}, indicating that all measured land uses fall within the very rapid infiltration class (>254 mm h^{-1}) according to standard soil infiltration classifications. (Anderson et al., 2020). Across various land uses in the Kalisari watershed, soil infiltration rates are categorized as very fast, with values exceeding 254 mm h^{-1}, in line with findings by (Hawari, 2020). Higher infiltration rates signify enhanced water absorption and storage capabilities within the land, reflecting improved land suitability (Fu et al., 2019).

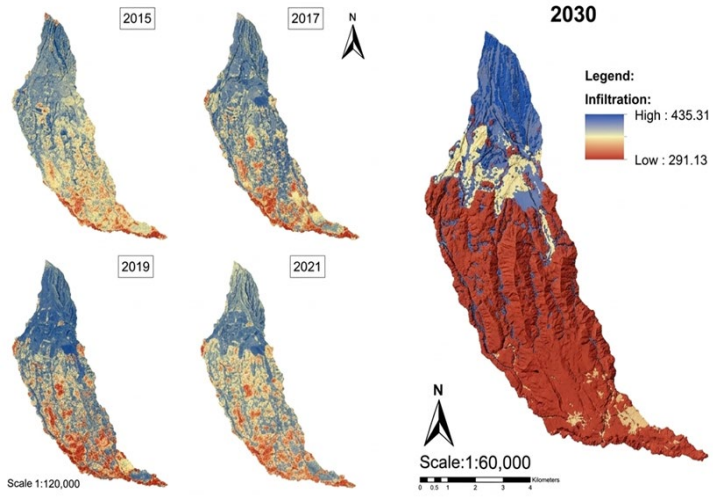

Figure 6: Prediction of soil infiltration rate (mm h-1) in Sub watershed Kalisari

According to Figure 6, despite falling within the "good infiltration" category as defined by (Mathur and Damle, 2021), the upstream region of the Kalisari watershed exhibits notably higher infiltration values compared to its downstream counterpart. This discrepancy can be attributed to the prevailing land use patterns in each area. The upstream segment is predominantly characterized by natural forest land, mahogany-coffee agroforestry, and pine-coffee agroforestry, contributing to its superior infiltration rates. Conversely, the middle and downstream areas are primarily occupied by dry land, paddy fields, and settlements, which exhibit comparatively lower infiltration rates. The substantial infiltration rate observed in rice field land use by 2030 can be attributed to various factors such as soil properties, alterations in cropping patterns, and shifts in agricultural land uses. Notably, changes in cropping patterns may render soils within the Kalisari sub-watershed less saturated due to intensive land management practices, thereby bolstering infiltration rates.

3.6 Characteristics and relationship of soil properties-soil infiltration

Soil texture across various land uses shows differences in the distribution of sand, silt, and clay particles, with a tendency toward sand (locations P1 and P2) and clay (locations P3, P4, and P5) as the dominant factor. The increase in clay particles is evident in increasingly intensive land uses, such as dryland and paddy fields. This is consistent with increases in soil bulk density (1.02 g cm-3) and aggregate stability (60.20 MWD), but leads to decreases in soil porosity (51.02%) and permeability (4.88 cm h-1). Organic matter is closely related to land use due to its relationship to litter input, which is a source of organic matter. However, it is noteworthy that the study area, which is an agricultural area and also applies organic fertilizer, found that the paddy fields (P5) had a higher organic matter content than the annual shrub (P3) and seasonal dryland (P4), at 2.22%.

According to projections, the expansion of shrubland and dryland areas until 2030 may slightly reduce infiltration capacity due to changes in soil structure and surface cover. However, the projected infiltration values remain well above the threshold for rapid infiltration (>254 mm h^{-1}), suggesting that the hydrological function of the soil remains relatively stable. In the Kalisari Sub-Watershed, precipitation and groundwater deposits serve as primary sources of water resources, with the infiltration process significantly influencing water supply on land.

Correlation and regression analyses revealed that soil physical properties, including bulk density (r = -0.57), porosity (r = 0.59), and aggregate

stability (r = -0.50), exerted notable effects on soil infiltration rates across various land uses in the Kalisari sub-watershed. Porosity emerged as the soil property most closely correlated with infiltration rate, exhibiting a positive relationship (y = 6.56x + 27.31), wherein an increase in soil pore percentage corresponded to enhanced infiltration.

The prevalence of dry land use, encompassing both seasonal and annual varieties, within the Kalisari sub-watershed has contributed to the prevalence of soils characterized by stable aggregate conditions, which in turn influence bulk density. Decreases in soil density correspond to increases in infiltration rates. Soil porosity plays a fundamental role in supporting air and water storage essential for soil biota life. The density of vegetation and root networks within the soil contributes significantly to pore space availability, particularly in agroforestry-based land uses characterized by dense vegetation and trees. Consequently, such areas exhibit higher infiltration capacities, as evidenced by the robust relationship between porosity and infiltration.

Aggregate stability also plays a critical role in determining water retention capacity, as explained by (Ren et al., 2020). Loose soil aggregates are less stable against external forces, facilitating easier water movement and potentially affecting water holding capacity. This underscores the importance of monitoring soil stability to ensure effective water retention within the soil profile.

Conclusion

The presence of influencing factors, particularly accessibility, plays a significant role in driving land use changes. Throughout the dynamic shifts observed from 2015 to 2021, there was a discernible decline in soil infiltration rates across agricultural lands within the Kalisari sub-watershed. These lands were originally categorized with very rapid infiltration, ranging between 379.34–397.27 mm h-1 (>254 mm h-1). However, upon modeling the projected distribution of soil infiltration rates for agricultural land in 2030, no substantial decrease in the forecasted infiltration rate was observed. Despite an increase in the area allocated to dryland, signaling intensified land cultivation and associated alterations in soil properties, this surge did not lead to a significant reduction in infiltration rates. Thus, it can be concluded that the Kalisari Sub-watershed is projected to remain capable of supporting agricultural activities in 2030, as the modeled infiltration rates remain within the very rapid infiltration category (>254 mm h^{-1}) despite moderate land use changes. Although minor variations in infiltration are expected due to land use changes, the projected values remain within a narrow range (approximately 380–400 mm h^{-1} ±5–10% uncertainty), indicating that the overall hydrological capacity of the watershed soils is likely to remain stable under the projected land use scenario.

References

Anderson, R. L., Brye, K. R., and Wood, L. S., 2020. Landuse and soil property effects on infiltration into Alfisols in the Lower Mississippi River Valley, USA. Geoderma Regional, 22, e00297. https://doi.org/10.1016/j.geodrs.2020.e00297.

Asra, R., Mappiasse, M. F., and Nurnawati, A. A., 2020. Penerapan Model CA-Markov Untuk Prediksi Perubahan Penggunaan Lahan Di Sub-DAS Bila Tahun 2036. AGROVITAL : Jurnal Ilmu Pertanian, 5,1, 1. https://doi.org/10.35329/agrovital.v5i1.630.

Besar, U. S. S., Ayu, I. W., and Soemarno, S. P., 2013. Assessment of Infiltration Rate under Different Drylands Types in. 3,10, Pp. 71–77.

Binte Mostafiz, R., Noguchi, R., and Ahamed, T., 2021. Agricultural land suitability assessment using satellite remote sensing-derived soil-vegetation indices. Land, 10,2, 223.

Dimara, A., Hamuna, B., and Bay, H., 2020. Pemanfaatan Citra Satelit Sentinel-2A Untuk Pemetaan Habitat Dasar Perairan Dangkal (Studi Kasus: Teluk Humbolt , Kota Jayapura). Jurnal Ilmu Kelautan Dan Perikanan Papua, 3,1, Pp. 25–31. https://doi.org/10.31957/acr.v3i1.1213.

Fardani, I., Mohmed, F. A. J., and Chofyan, I., 2020. Pemanfaatan Prediksi Tutupan Lahan Berbasis Cellular Automata-Markov dalam Evaluasi Rencana Tata Ruang. MKG, 21,2, Pp. 157–169.

Fransiska, B., and Pratomoatmojo, N. A., 2019. Prediksi Perkembangan Permukiman Berbasis Cellular Automata dengan Batasan Kawasan Rawan Banjir di Perkotaan Kabupaten Bojonegoro. Jurnal Teknik ITS, 8,2, Pp. 116–122.

Fu, Q., Hou, R., Li, T., Li, Y., Liu, D., and Li, M., 2019. A new infiltration model for simulating soil water movement in canal irrigation under laboratory conditions. 213 October 2018, Pp. 433–444. https://doi.org/10.1016/j.agwat.2018.10.021.

Hawari, S. D., 2020. Analisis Tingkat Laju Infiltrasi Pada Sub Daerah Aliran Sungai (Das) Kampar Outlet Rimbo Panjang. 7, Pp. 1–9.

Indarto, I., Mandala, M., Febrian Arifin, F., and Lukman Hakim, F., 2020. Aplikasi Citra Sentinel-2 Untuk Pemetaan Tutupan Dan Peruntukan Lahan Pada Tingkat Desa. Jurnal Geografi, 12,02, 189. https://doi.org/10.24114/jg.v12i02.16970.

Iserloh, T., Ries, J., Arnáez, J., Boix-Fayos, C., Butzen, V., Cerdà, A., Echeverría, M., Fernández-Gálvez, J., Fister, W., and Geißler, C., 2013. European small portable rainfall simulators: A comparison of rainfall characteristics. Catena, 110, Pp. 100–112.

Islam, H., Abbasi, H., Karam, A., Chughtai, A. H., and Ahmed Jiskani, M., 2021. Geospatial analysis of wetlands based on land use/land cover dynamics using remote sensing and GIS in Sindh, Pakistan. Science Progress, 104,2, 00368504211026143.

Ji, X., Thompson, A., Lin, J., Jiang, F., Ge, H., Yu, M., and Huang, Y., 2020. Modeling spatial distribution of rainfall infiltration amounts in South China using cellular automata and its relationship with the occurrence of collapsing gullies. Catena, 194, Pp. 104676.

Kusrini, Suharyadi, and Hardoyo, S. R., 2016. Perubahan Penggunaan Lahan dan Faktor yang Mempengaruhinya di Kecamatan Gunungpati Kota Semarang. Majalah Geografi Indonesia, 25,1, Pp. 25–40. https://doi.org/10.22146/mgi.13358.

Ma, L., Wang, N., Liu, Y., Zhao, Y., Han, Q., Wang, X., Woolliams, E. R., Bouvet, M., Gao, C., and Li, C., 2021. An in-flight radiometric calibration method considering adjacency effects for high-resolution optical sensors over artificial targets. IEEE Transactions on Geoscience and Remote Sensing, 60, Pp. 1–13.

Machiwal, D., Jha, M. K., and Mal, B. C., 2006. Modelling Infiltration and quantifying Spatial Soil Variability in a Wasteland of Kharagpur, India. Biosystems Engineering, 95,4, Pp. 569–582. https://doi.org/10.1016/j.biosystemseng.2006.08.007.

Mao, Z.-H., Deng, L., Duan, F.-Z., Li, X.-J., and Qiao, D.-Y., 2020. Angle effects of vegetation indices and the influence on prediction of SPAD values in soybean and maize. International Journal of Applied Earth Observation and Geoinformation, 93, 102198.

Mathur, U., and Damle, R., 2021. Impact of air infiltration rate on the thermal transmittance value of building envelope. Journal of Building Engineering, 40 November 2020, 102302. https://doi.org/10.1016/j.jobe.2021.102302.

McHugh, M. L., 2012. Lessons in biostatistics interrater reliability: The kappa statistic. Biochemica Medica, 22,3, Pp. 276–282.

Morbidelli, R., Corradini, C., Saltalippi, C., Flammini, A., Dari, J., and Govindaraju, R. S., 2018. Rainfall infiltration modeling: A review. Water (Switzerland), 10,12. https://doi.org/10.3390/w10121873.

Morrison, C. M., Betancourt, W. Q., Quintanar, D. R., Lopez, G. U., Pepper, I. L., and Gerba, C. P., 2020. Potential indicators of virus transport and removal during soil aquifer treatment of treated wastewater effluent. Water Research, 177, Pp. 115812.

Morsy, S., and Mashaan, H., 2022. Impact of land use/land cover on land surface temperature and its relationship with spectral indices in Dakahlia Governorate, Egypt. International Journal of Engineering and Geosciences, 7,3, Pp. 272–282.

Munthali, M., Mustak, S., Adeola, A., Botai, J., Singh, S., and Davis, N., 2020. Modelling land use and land cover dynamics of Dedza district of Malawi using hybrid Cellular Automata and Markov model. Remote Sensing Applications: Society and Environment, 17, 100276.

Nita, I., Ayuningtyas, P., Prijono, S., and Putra, A. N., 2024. ANALISIS KAPASITAS INFILTRASI LAHAN PERTANIAN DI SUB DAS KALISARI, MALANG. Jurnal Tanah Dan Sumberdaya Lahan, 11,1, Pp. 117–123.

Norizah, K., Jamhuri, J., Balqis, M., Mohd Hasmadi, I., and Nor Akmar, A., 2022. Land Use and Land Cover Change Prediction Using ANN-CA Model. In Tropical Forest Ecosystem Services in Improving Livelihoods For Local Communities, Pp. 107–125. Springer.

Pérez-Girón, J. C., Díaz-Varela, E. R., and Álvarez-Álvarez, P., 2022. Climate-driven variations in productivity reveal adaptive strategies in Iberian cork oak agroforestry systems. Forest Ecosystems, 9. https://doi.org/10.1016/j.fecs.2022.100008.

Rahmasari, A. N., and Rustanto, A., 2022. ESTIMATION OF OIL PALM PLANT PRODUCTIVITY USING SENTINEL-2A IMAGERY AT CIKASUNGKA PLANATION PTPN VIII, BOGOR, WEST JAVA. International Journal of Remote Sensing and Earth Sciences (IJReSES), 19,1, Pp. 31–38.

Ren, X., Hong, N., Li, L., Kang, J., and Li, J., 2020. Effect of infiltration rate changes in urban soils on stormwater runoff process. Geoderma, 363 August 2019. https://doi.org/10.1016/j.geoderma.2019.114158.

Saputra, N. E., Wibowo, C., and Lisnawati, Y., 021. Analysis of soil physical properties and infiltration rates for various landuses at Gunung Dahu Research Forest, Bogor District, West Java Province. IOP Conference Series: Earth and Environmental Science, 713(1). https://doi.org/10.1088/1755-1315/713/1/012034.

Sun, D., Yang, H., Guan, D., Yang, M., Wu, J., Yuan, F., Jin, C., Wang, A., and Zhang, Y., 2018. The effects of land use change on soil infiltration capacity in China: A meta-analysis. Science of The Total Environment, 626, Pp. 1394–1401. https://doi.org/10.1016/j.scitotenv.2018.01.104.

Tamod, C. J. K. T., Aryanto, R., and Purwiyono, T. T., 2020. Analisis Laju Infiltrasi Berbagai Penggunaan Lahan. Indonesian Mining and Energy Journal, 3,2, Pp. 76–88.

Tariq, A., Riaz, I., Ahmad, Z., Yang, B., Amin, M., Kausar, R., Andleeb, S., Farooqi, M. A., and Rafiq, M., 2020. Land surface temperature relation with normalized satellite indices for the estimation of spatio-temporal trends in temperature among various land use land cover classes of an arid Potohar region using Landsat data. Environmental Earth Sciences, 79,1, Pp. 1–15.

Thomas, A.-D., Ofosu, A. E., Emmanuel, A., De-Graft, A. J., Ayine, A. G., Asare, A., and Alexander, A., 2020. Comparison and estimation of four infiltration models. Open Journal of Soil Science, 10,2, Pp. 45–57.

Verma, P., Raghubanshi, A., Srivastava, P. K., and Raghubanshi, A., 2020. Appraisal of kappa-based metrics and disagreement indices of accuracy assessment for parametric and nonparametric techniques used in LULC classification and change detection. Modeling Earth Systems and Environment, 6,2, Pp. 1045–1059.

Wang, L., Zhong, C., Gao, P., Xi, W., and Zhang, S., 2015a. Soil Infiltration Characteristics in Agroforestry Systems and Their Relationships with the Temporal Distribution of Rainfall on the Loess Plateau in China. PLOS ONE, 10,4, e0124767. https://doi.org/10.1371/journal.pone.0124767.

Wang, L., Zhong, C., Gao, P., Xi, W., and Zhang, S., 2015b. Soil infiltration characteristics in agroforestry systems and their relationships with the temporal distribution of rainfall on the loess plateau in China. PLoS ONE, 10,4, Pp. 1–12. https://doi.org/10.1371/journal.pone.0124767.

Wicaksono, K. S., Nita, I., Putra, A. N., Widianto, W., Rusdianto, F. H., and Ayuningtyas, P., 2022). Effect of Land Cover Differences on Soil Infiltration at UB Forest, Karangploso Malang. Jurnal Tanah Dan Sumberdaya Lahan, 9,1, Pp. 131–139. https://doi.org/10.21776/ub.jtsl.2022.009.1.14

Zokaib, S., and Naser, G., 2012. A study on rainfall, runoff, and soil loss relations at different landuses—A case in Hilkot watershed in Pakistan. International Journal of Sediment Research, 27,3, Pp. 388–393. https://doi.org/10.1016/S1001-6279(12)60043-2